Geotechnical assessment and numerical modeling of Pit-3 at Khan Altai deposit

Sodnom B.[1], Battulga G.[1], Ganbold B.[2], Myanganbayar D.[2]
[1]Trigteq LLC, [2]Khan Altai Resources LLC

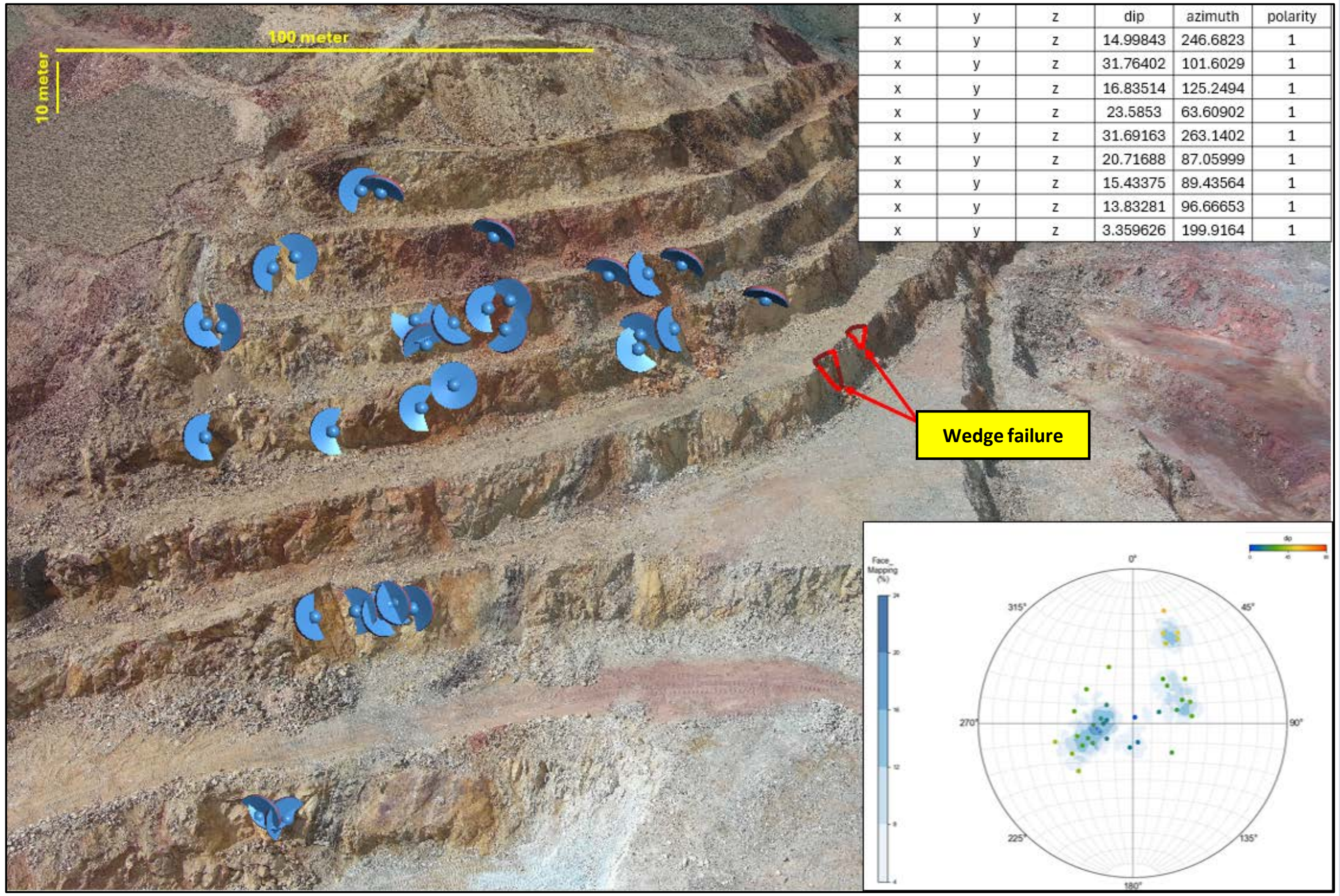

x	y	z	dip	azimuth	polarity
x	y	z	14.99843	246.6823	1
x	y	z	31.76402	101.6029	1
x	y	z	16.83514	125.2494	1
x	y	z	23.5853	63.60902	1
x	y	z	31.69163	263.1402	1
x	y	z	20.71688	87.05999	1
x	y	z	15.43375	89.43564	1
x	y	z	13.83281	96.66653	1
x	y	z	3.359626	199.9164	1

Face mapping – Collection of structural elements

Deposit location and Geological setting

- The Khan-Altai deposit is a gold deposit located in Gobi-Altai Province, within the Neoproterozoic–Cambrian terrane. The deposit is mainly composed of andesitic tuff, basalt, limestone, rhyolite, rhyolitic tuff, siltstone, tuff, and tuff breccia.

- Mineralization is associated with quartz–sericite–sulfide alteration within the volcanic rocks, and the deposit's geology and ore distribution are primarily controlled by the Tsakhir and Bööriin Am faults.

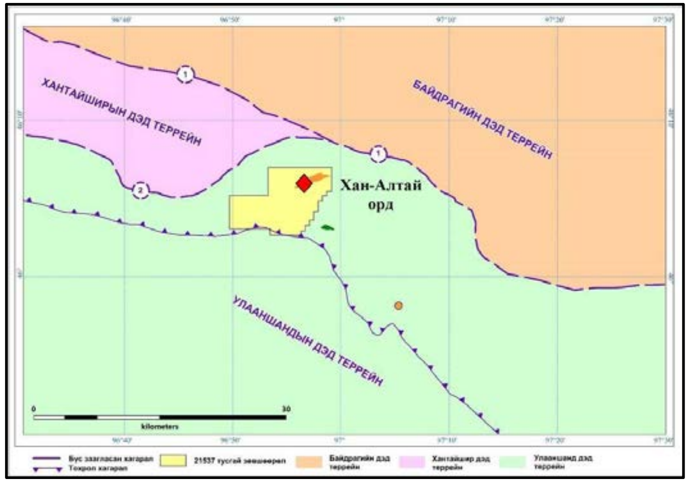

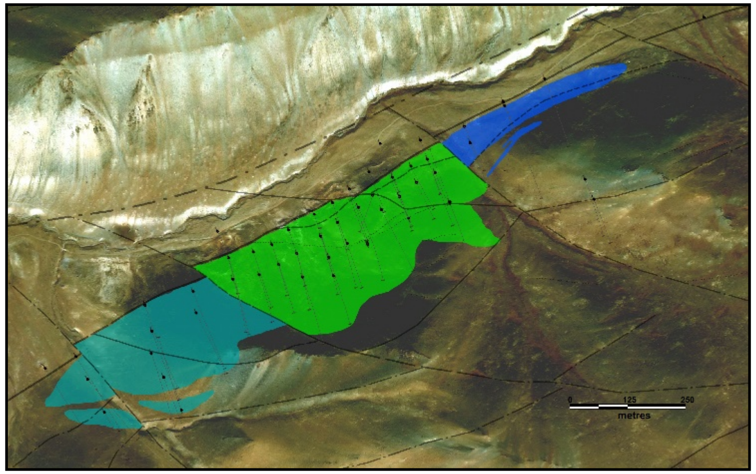

Location, Plan View, and Geological Context of Pit-3

Research Objectives, Data Screening, and Workflow

The study is based on quality-screened data and a staged geotechnical workflow.

- **Objective:** To provide an integrated assessment of the geotechnical conditions, rock mass quality, and 2D stability of representative sections at Pit-3, and to incorporate fracture network modelling and 3D analysis. Following data screening, 18 of the 120 drillholes were selected as suitable for use in the assessment.

- **Workflow:** RMR89/GSI assessment → parameter estimation → solid modelling → validation using LEM and FEM.

Key message: The study results are based on data from 18 screened drillholes; therefore, the interpretation is directly dependent on the quality of the available data.

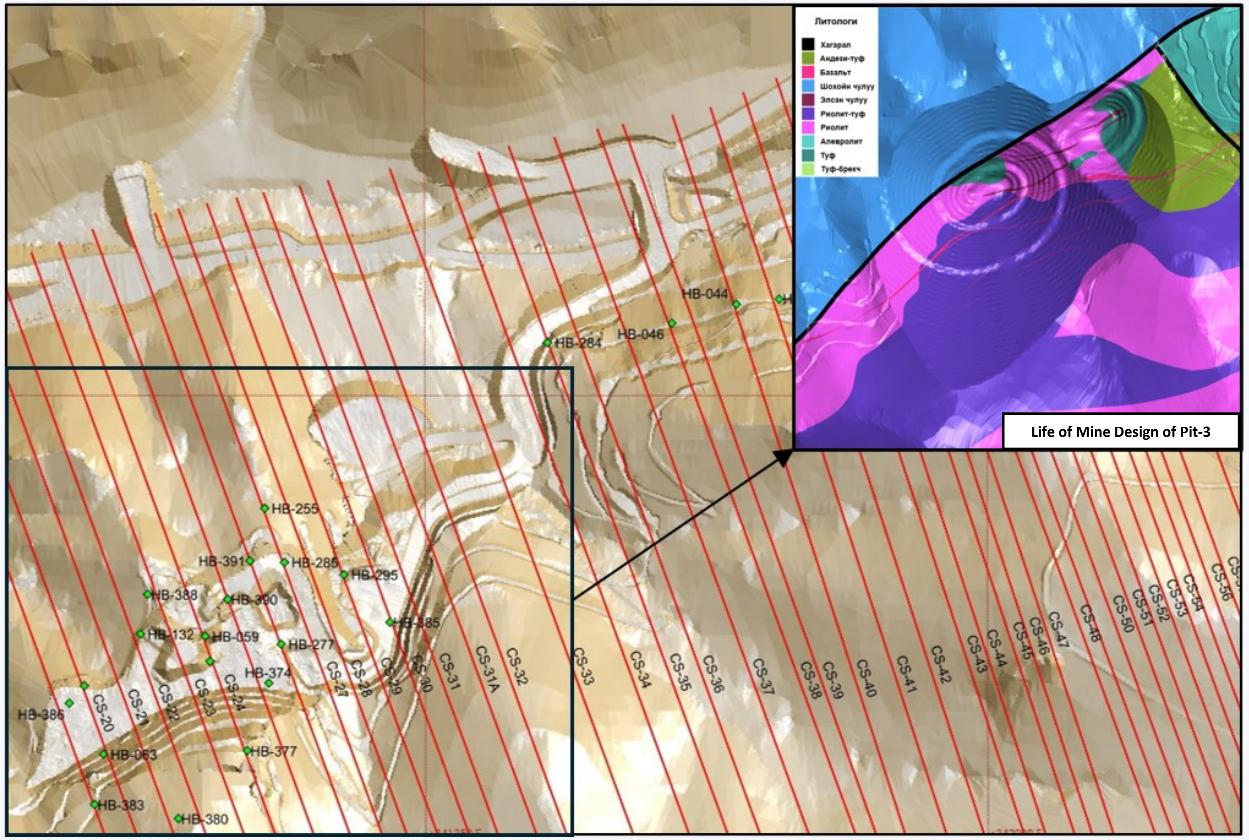

Geological Model of Pit-3

Data screening → Rock mass classification → Parameter estimation → Spatial modelling & DFN → **2D, 3D analysis of rock mass input LEM + FEM/SRF**

Geotechnical condition

The key site-specific factors controlling slope stability are summarized below.

- No groundwater was encountered between elevations 2480 and 2600 m; however, fracture-controlled seepage may increase with depth.
- RMR values ranging from 29 to 56 indicate that the rock mass is blocky and fractured, with unevenly distributed quality.
- Clayey material (CLY) is the dominant discontinuity infill, creating conditions that may reduce shear resistance along the discontinuities.
- Discontinuity surfaces are generally slightly rough, increasing the potential for sliding and wedge failure.

Clay-filled, slightly rough discontinuities weaken the rock mass and increase the potential for sliding.

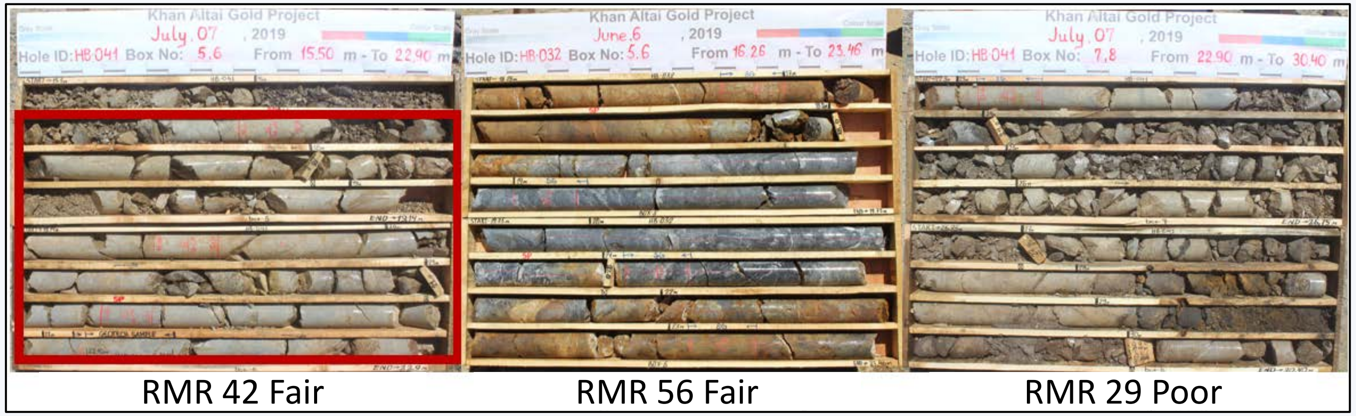

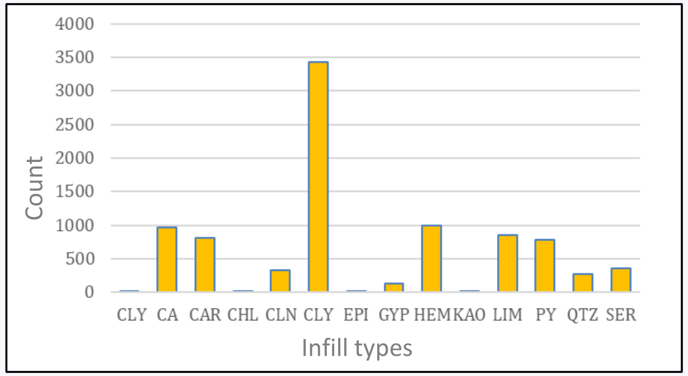

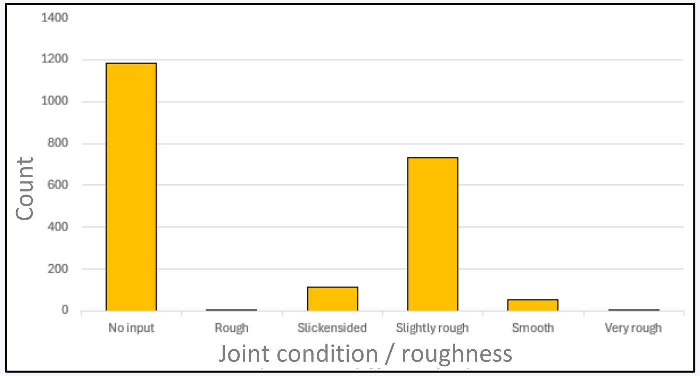

Photographs Showing Site Conditions, Failure Features, and Rock Conditions

Rock Quality Designation

Core **logging**

- RQD and geotechnical logs along the drillholes indicate that the rock mass is heterogeneous and blocky.
- Variations in RQD indicate high fracture intensity and a high frequency of structural discontinuities.

Based on the RQD assessment, the rock mass has a fractured, blocky structure.

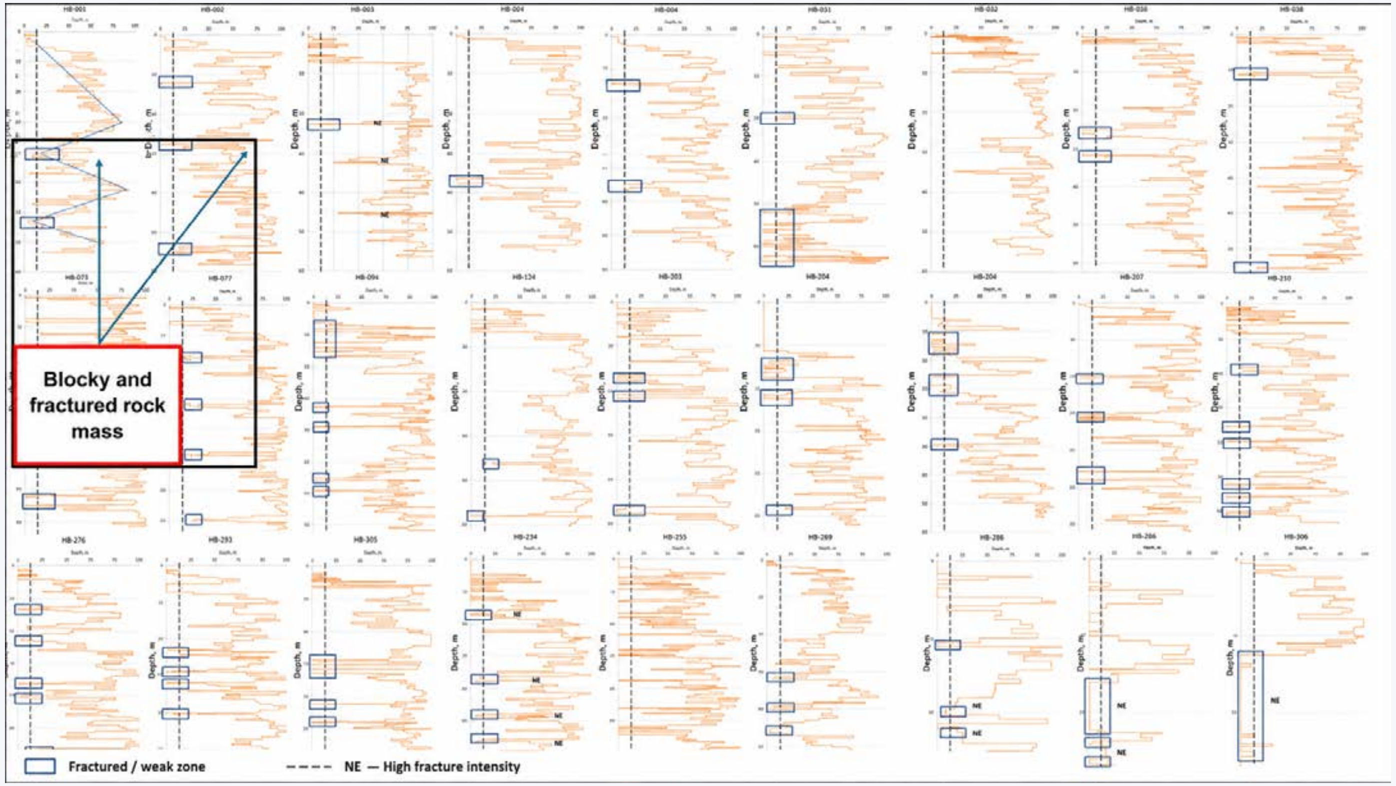

RQD, structural information

Structural Analysis of Discontinuities

Face mapping

- The stereonet developed from drillhole data did not clearly define the distribution of discontinuity orientations. Therefore, face mapping was conducted to more accurately determine the actual orientations and spatial distribution of the discontinuities.

- The face-mapping results produced more distinct discontinuity sets on the stereonet, allowing the structural pattern to be defined with greater confidence.

By incorporating face-mapping data, the discontinuity orientations were characterized more realistically, improving the reliability and accuracy of the stereonet analysis.

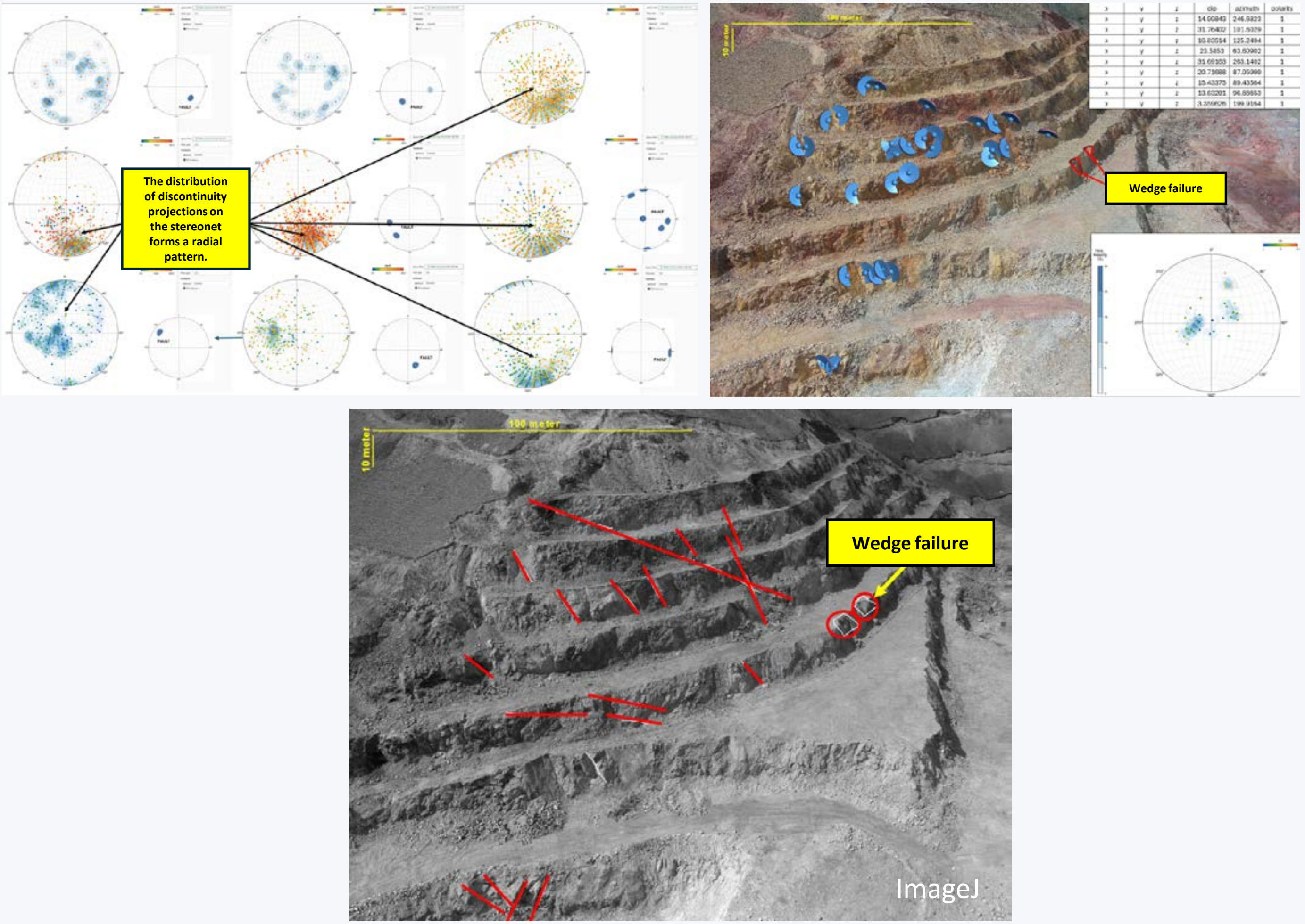

Структурын мэдээлэл

Distribution of RMR89 classification estimation

- Bieniawski's RMR89 classification was calculated based on the geotechnical logs from 18 drillholes.
- The minimum, average, and maximum values vary between lithologies, indicating substantial spatial variability in rock mass quality.
- Although the average values generally fall within the fair-to-good range, the minimum values clearly identify zones of poor-quality rock mass.

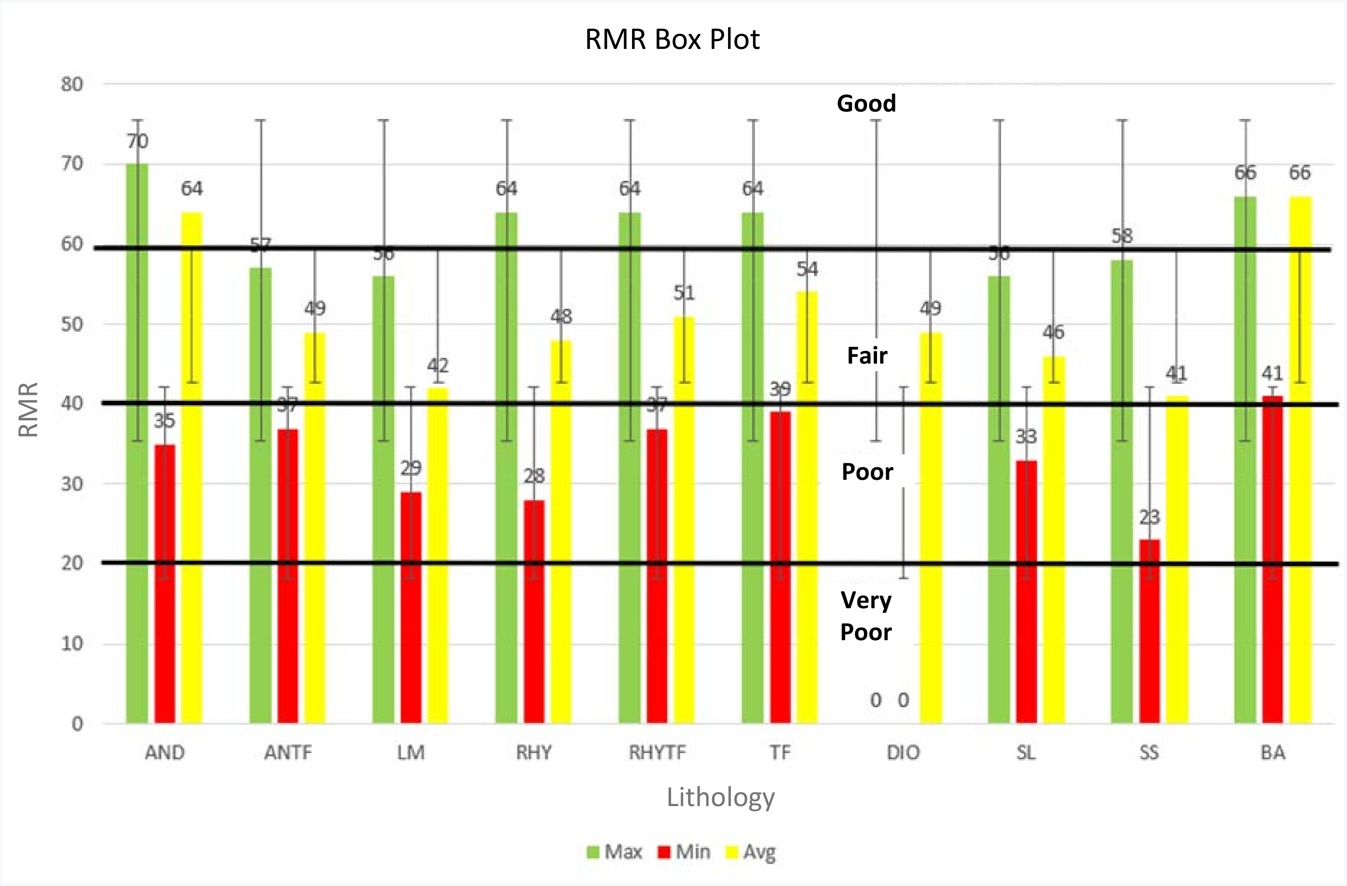

Rock Mass Classification

Variogram

Geotechnical modelling & variogram configuration

The spatial distribution of rock mass quality was modelled using RMR values.

- Drillhole intervals were length-weighted, resulting in a geotechnical composite interval length of 2.77 m.
- Spatial continuity was evaluated, and the optimal interpolation range was determined to be approximately 90 m (90.77 m).
- Ellipsoidal search parameters were defined for each domain to represent the orientation and extent of spatial continuity.
- The interpolation was constrained to the extent of the drillhole data, and the model was calibrated against the actual geotechnical logging data.

The spatial continuity parameters were derived from the analysis, and the geotechnical model was calibrated against the available field data.

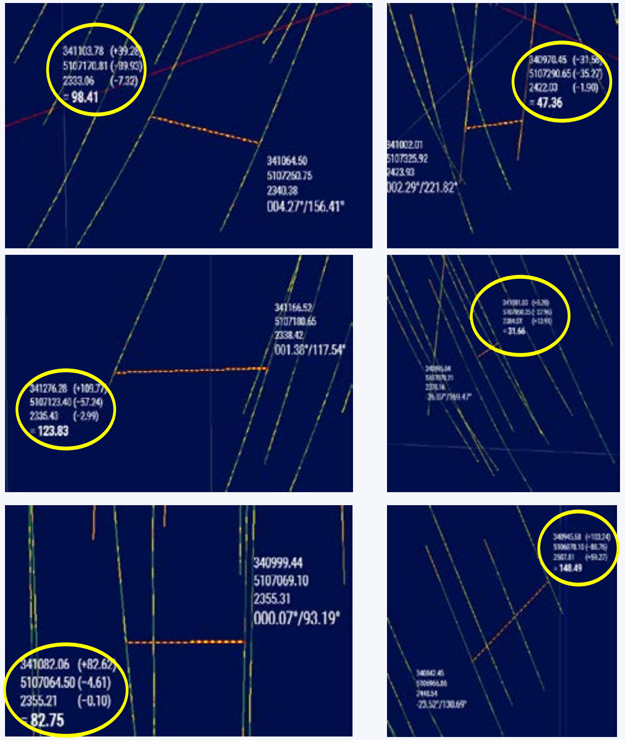

Main Variogram Parameters		BA Domain Variogram Parameters	
Shape	Ellipsoid	Shape	Ellipsoid
Dip angle	34.5°	Dip angle	35.5°
Elongation direction	125°	Elongation direction	15.5°
Dip azimuth	0°	Dip azimuth	90°
Variance	152	Variance	51.1
Sill value	42.3	Sill value	65.5
Nugget value	10	Nugget value	2
L:W:H	300:250:100	L:W:H	90:90:20
Base range	90	Base range	90
Optimization	0.3	Optimization	0.3
Alpha	9	Alpha	3
LM Domain Variogram Parameters		**MAS Domain Variogram Parameters**	
Shape	Ellipsoid	Shape	Ellipsoid
Dip angle	0°	Dip angle	0°
Elongation direction	0°	Elongation direction	0°
Dip azimuth	90°	Dip azimuth	90°
Variance	131	Variance	69.3
Sill value	70.13	Sill value	25
Nugget value	2	Nugget value	5
L:W:H	500:150:25	L:W:H	500:300:2.8
Base range	120	Base range	90
Optimization	0.3	Optimization	0.3
Alpha	3	Alpha	3
MAS Domain Variogram Parameters		**RHY Domain Variogram Parameters**	
Shape	Ellipsoid	Shape	Ellipsoid
Dip angle	34.5°	Dip angle	0°
Elongation direction	0°	Elongation direction	0°
Dip azimuth	125°	Dip azimuth	90°
Variance	83.6	Variance	85.3
Sill value	42.36	Sill value	82.67
Nugget value	10	Nugget value	0.3
L:W:H	300:250:99.4	L:W:H	119:180:2.8
Base range	90	Base range	90
Optimization	0.3	Optimization	0.3
Alpha	9	Alpha	3

Variogram input parameters

Rock mass classification model

- The rock mass classification values were composited and averaged, then spatially interpolated between drillholes using an implicit modelling method.
- The model incorporated the Tsakhir Fault, lithological boundaries, and the Pit-3 mine geometry, allowing the spatial distribution to reflect the actual geological setting.
- This approach enabled the spatial variation in rock mass quality to be represented and allowed zones of poor and relatively good rock mass quality to be distinguished.
- The resulting model was used as the basis for geotechnical analysis and slope stability assessment.

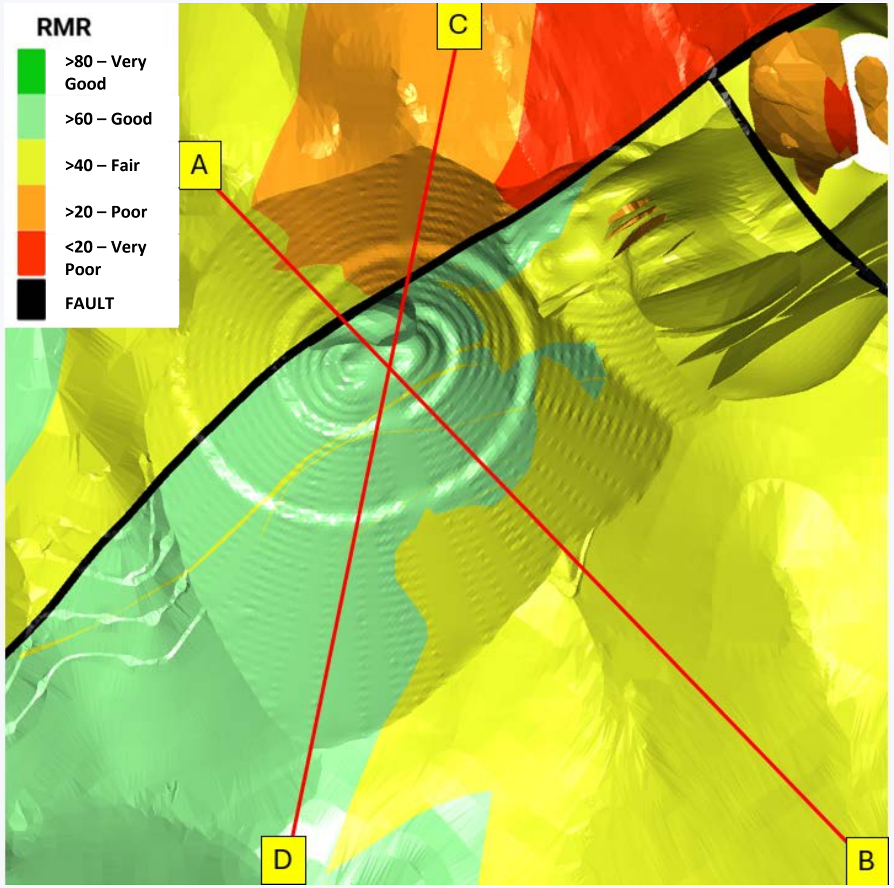

Rock mass classification model

2D Stability – LEM

The Bishop, Janbu, and Morgenstern–Price methods were compared along the A–B and C–D sections.

- For the A–B section, the factor of safety of the north wall ranges from approximately 1.12 to 1.24, indicating that it is close to the limiting equilibrium condition. In contrast, the south wall values range from 1.65 to 1.82, indicating relatively stable conditions.
- For the C–D section, the factor of safety of the south wall ranges from 1.41 to 1.56, indicating stable conditions, whereas the north wall values range from approximately 1.09 to 1.20, indicating conditions close to limiting equilibrium.
- The Bishop result of 0.102 for the south wall of the C–D section is inconsistent with the results obtained using the other methods and differs substantially from the expected field conditions. It was therefore treated as an outlier and was not used independently in the interpretation.

A–B

North wall — close to limit equilibrium

C–D

The unmatching Bishop result did not affect the overall interpretation.

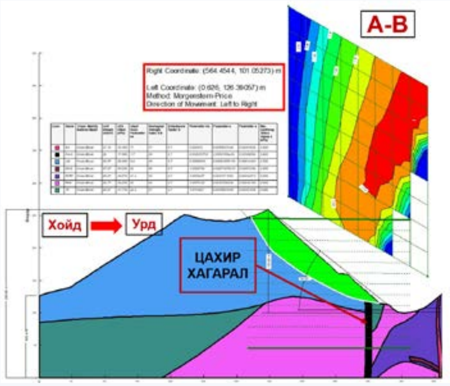

Figure 1. A-B section, Morgenstern-Price method, displacement direction L-R

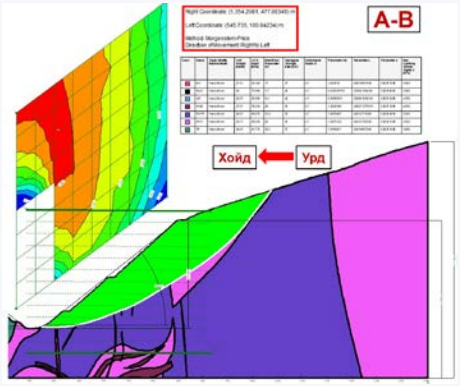

Figure 2. A-B section, Morgenstern-Price method, displacement direction Right to Left

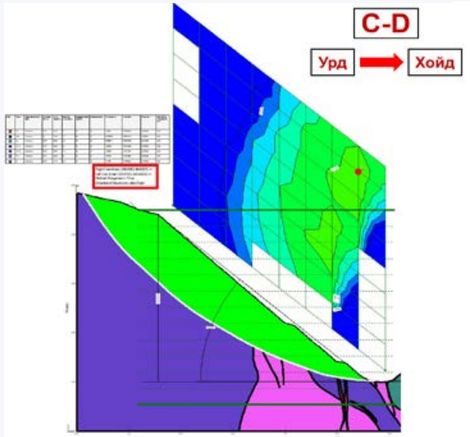

Figure 3. C-D section, Morgenstern-Price method, displacement direction Left to Right

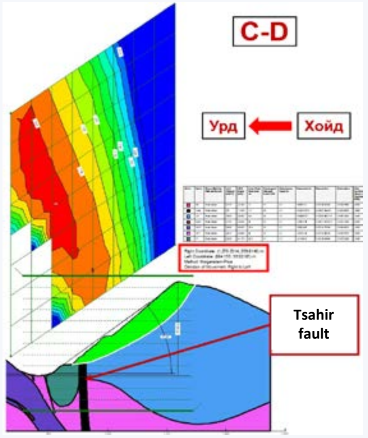

Figure 3. C-D section, Morgenstern-Price method, displacement direction Right to Left

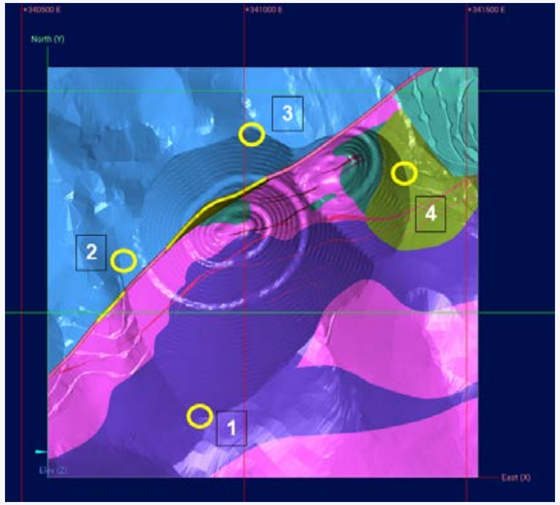

Critical LEM Slip Surfaces for the A–B and C–D Sections

2D Stability Results – FEM/SRF

Strength reduction analysis was used to verify the critical zones identified by the LEM analyses through their displacement and deformation responses.

- For the A–B section, the critical SRF was approximately 1.03 for the north wall and 1.52 for the south wall.
- For the C–D section, the critical SRF was approximately 1.30 for the south wall and 1.00 for the north wall, indicating that the north wall is close to the limiting stability condition.
- As the strength reduction factor increased, total displacement gradually increased, followed by a sharp rise as the critical SRF was approached.
- Displacement increased relatively smoothly in the A–B section, whereas a stepwise increase was observed in the C–D section, indicating the influence of geological structures.
- The Tsakhir Fault controls the response of the north wall, while the basalt dyke influences the south wall, resulting in different stability performances.

1.032
A–B North

1.515
A–B South

5 – 7.5 мм
Critical displacement

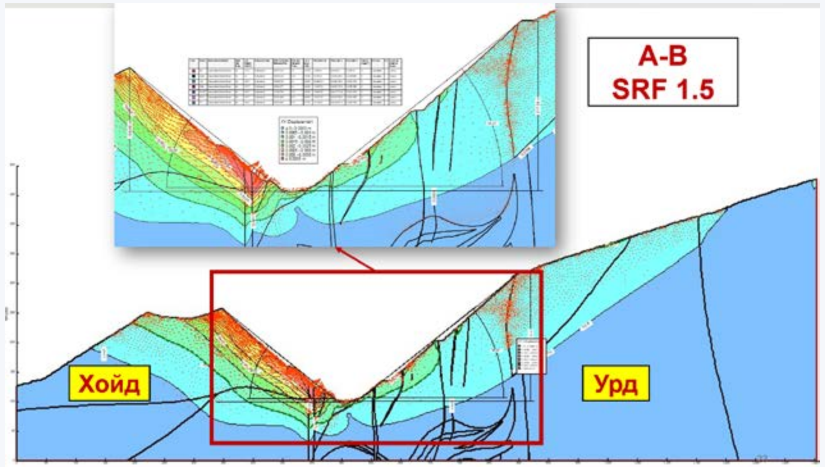

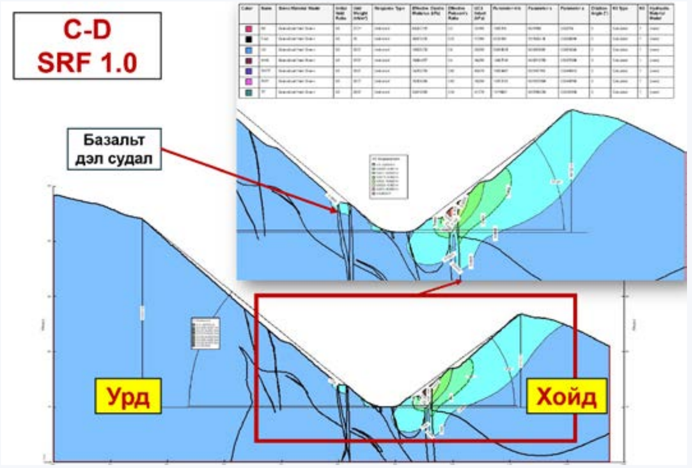

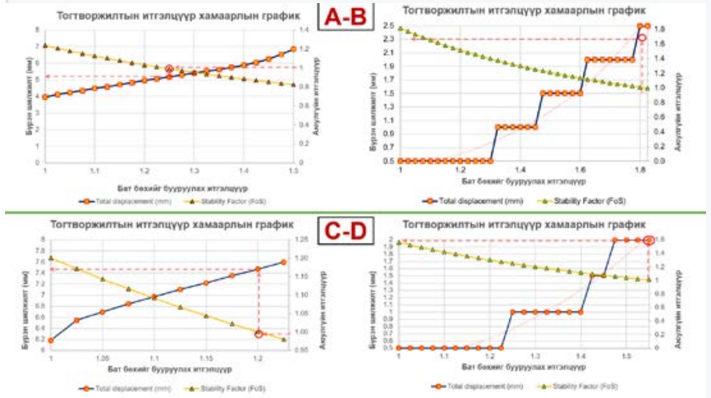

Geotechnical Simulation and Analysis Results Along Section A-B

Analysis Direction	Mine Slope Angle	Limit Equilibrium Analysis			Finite Element Analysis Strength Reduction Factor (SRF)
		Bishop	Janbu	Morgenstern–Price	
L–R NE100° (North wall)	38.8°	1.221	1.121	1.238	1.032 (Rel. FoS ≈ 1.2)
R–L SW190° (South wall)	38.4°	1.824	1.656	1.819	1.515 (Rel. FoS ≈ 1.2)

Geotechnical Simulation and Analysis Results Along Section C-D

Analysis Direction	Mine Slope Angle	Limit Equilibrium Analysis			Finite Element Analysis Strength Reduction Factor (SRF)
		Bishop	Janbu	Morgenstern–Price	
L–R SE135° (South wall)	40°	0.102	1.417	1.561	1.30 (Rel. FoS ≈ 1.2)
R–L NW315° (North wall)	37.5°	1.184	1.097	1.201	1.00 (Rel. FoS ≈ 1.2)

FEM/SRF Responses for the A–B and C–D Sections

Synthetic structural model

Fracture Distribution and Connectivity Intensity

- A three-dimensional discrete fracture network (DFN) was developed using the principal fracture sets identified within the Pit-3 area.
- Fracture orientation, size, and spatial distribution were modelled based on the available data, reproducing the observed structural distribution with an estimated agreement of approximately 80–90%.
- The network illustrates fracture intersections and connectivity, characterizing the blocky and fractured nature of the rock mass.
- **Objective:** To establish a baseline model for assessing structurally controlled failure mechanisms.
- **Outcome:** The fracture network and its spatial distribution were successfully modelled, allowing structural influences to be represented in a 3D environment.
- At the current stage, the DFN is not considered a result; rather, it is a development model intended for use in further analysis.

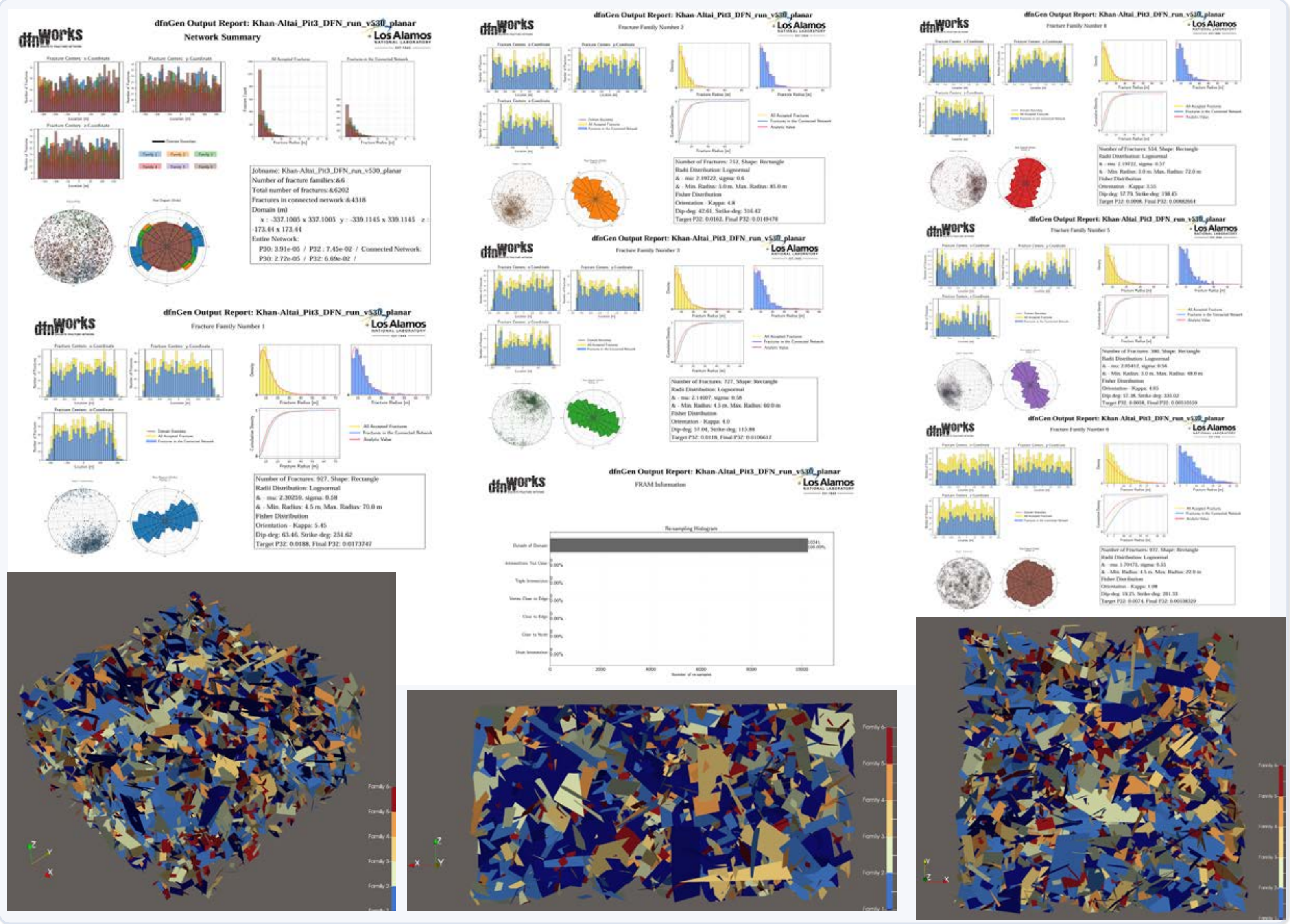

The fracture network was represented with a high degree of confidence and is suitable for use in 3D analysis.

3D Slope Stability Result - LEM

The baseline 3D search without the DFN illustrates the influence of geometry alone.

- The figure presents the results of a three-dimensional slip-surface search under baseline conditions, without considering the effects of discontinuities.
- The baseline analysis allows the effects of slope geometry, overall shape, and material properties to be evaluated independently.
- The results identify a zone with potential for wedge failure, with a factor of safety of approximately 0.88.

The analysis without the DFN identified one potential wedge failure case.

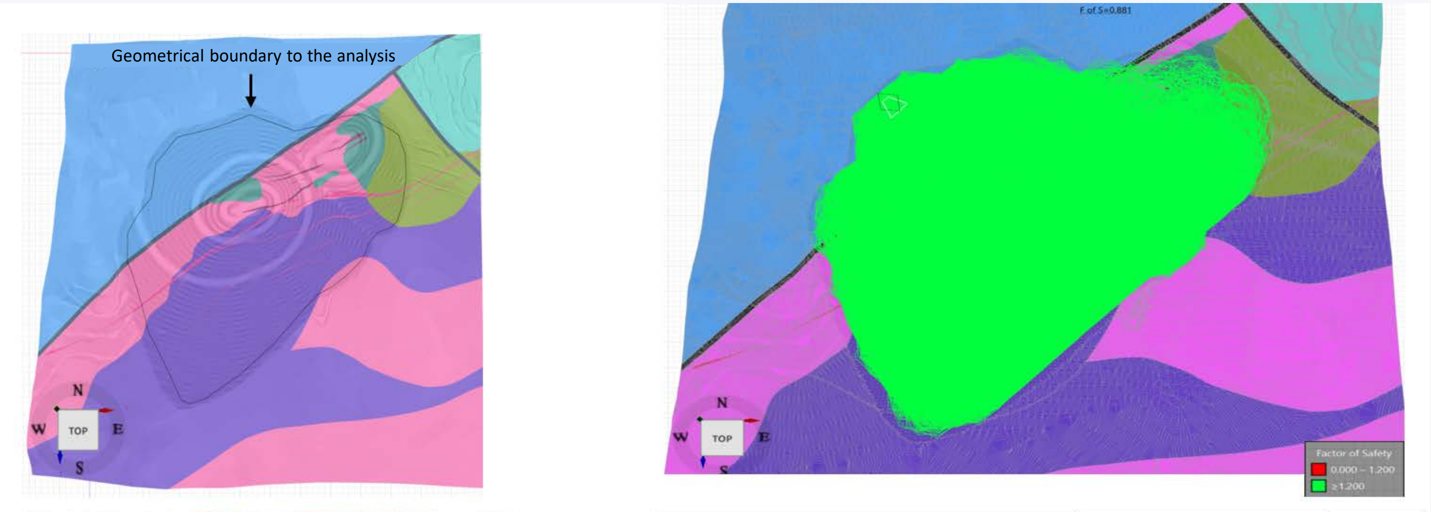

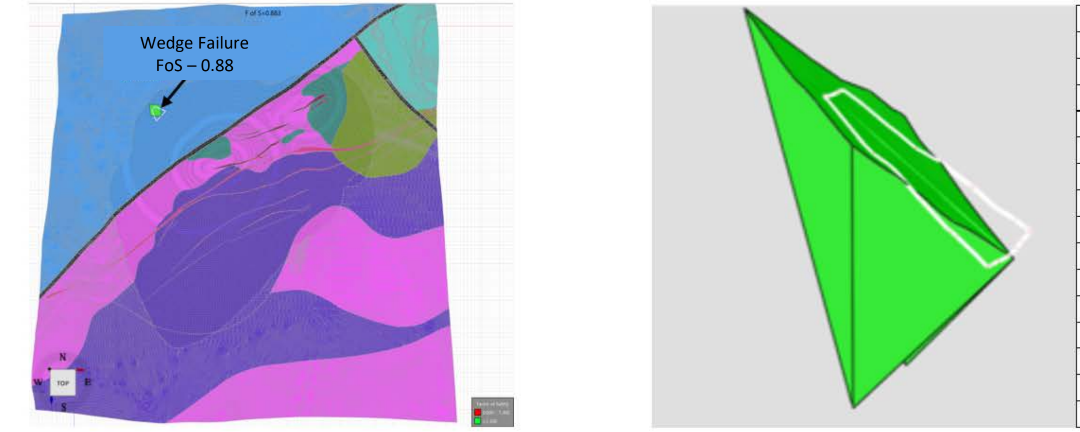

Sliding Direction (°)	137.85007
X (m)	262.5
Y (m)	197.64256
Z (m)	262.5
Volume (m³)	24,316.32
Weight (kN)	656,054.29
Effective Normal Stress (kPa)	111.70752
Cohesive Strength (kPa)	116.81418
Frictional Strength (kPa)	168.38376
Shear Mobilized (kPa)	323.78134
Total Normal Stress (kPa)	111.70752
Shear Resistance (kPa)	285.19794
Base Cohesion (kPa)	116.81418
Base Friction Angle (°)	56.439296
Friction Coefficient	1.5073629
Factor of safety	0.88

Slope stability analysis – without DFN

3D Slope Stability Result - LEM

The 3D search incorporating the DFN demonstrates the model's sensitivity to structural controls.

- When the DFN is incorporated, the slip geometry becomes sensitive to the orientation and spatial distribution of discontinuities, resulting in changes to the failure mechanism.
- Compared with the baseline condition, multiple potential wedge-failure blocks are identified, indicating that the failure mechanism is structurally controlled.
- The intersections and connectivity of discontinuities define the potential slip surfaces, creating conditions in which wedge failure becomes the dominant mechanism.
- These results provide a preliminary three-dimensional representation of how structural controls influence the failure mechanism.
- When interpreted together with the baseline analysis without the DFN, the structural influence becomes more clearly defined.

The inclusion of the DFN increases the number of potential wedge failures and clearly demonstrates, in three dimensions, that the failure mechanism is structurally controlled.

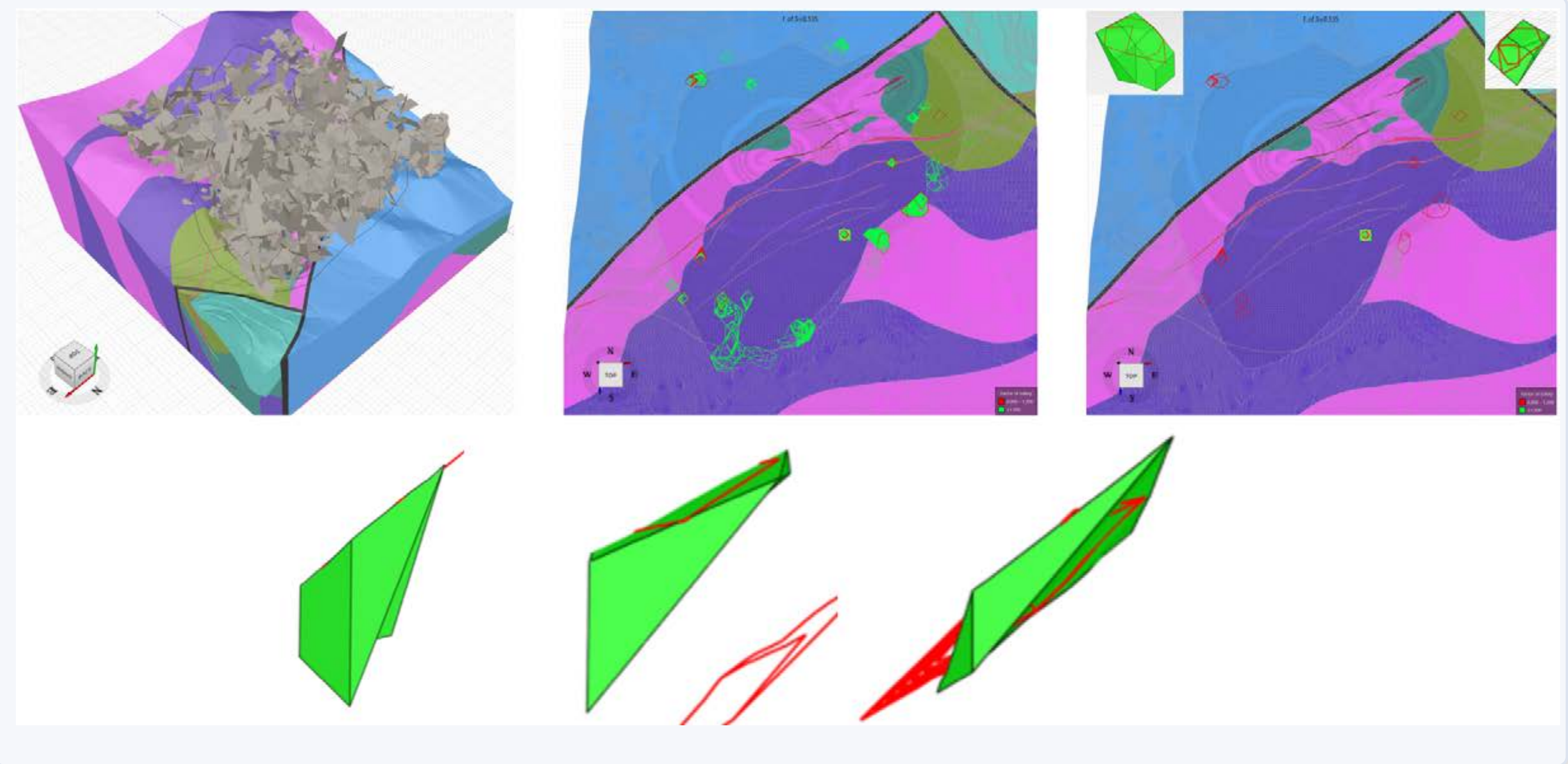

Slope stability analysis – with DFN

Conclusion and further investigation

Main conclusion

- A geotechnical model was developed based on data from 18 drillholes, with a composite interval length of 2.77 m and a spatial continuity range of approximately 90 m.
- The rock mass is blocky and fractured, with a heterogeneous distribution of RMR values.
- The 2D analyses produced lower FoS values for the north wall (1.09–1.24) and relatively higher values for the south wall (1.65–1.82).Slope stability is primarily influenced by the Tsakhir Fault on the north wall and the basalt dyke on the south wall.
- During strength reduction, displacement reached approximately 5 mm for section A–B and 7.5 mm for section C–D.
- The baseline 3D analysis identified several potential failure blocks.
- Incorporating the DFN increased the number of potential wedge failures and confirmed that the failure mechanism is structurally controlled.

Future research

- The probability of sliding and failure, together with the associated movement characteristics, should be assessed in greater detail.
- Additional data on rock mechanical properties, including strength and deformability, should be obtained.
- The frictional properties of the discontinuities should be determined.
- The rock mass classifications, including RMR and GSI, should be updated.
- Groundwater conditions and pore-water pressures should be measured.
- The in-situ stress state, including its orientation and magnitude, should be determined.
- Blast effects and slope displacement should be monitored.
- The three-dimensional analysis incorporating the Discrete Fracture Network (DFN) should be further developed.
- The mine slope geometry and final pit-limit design should be optimized.